

Sulfur-Bridged Co^{III}Pt^{II}Co^{III} Trinuclear Complexes with Mixed Aliphatic and Aromatic Thiolate Ligands: Effect of Nonbridging Ligands on the Homochiral Linkage of Cobalt(III) Octahedrons by Platinum(II)Masakazu Hirotsu,^{*†} Ryota Endo,[†] Takashi Yoshimura,[‡] and Takumi Konno^{*‡}

Department of Chemistry, Graduate School of Science, Osaka University, Toyonaka, Osaka 560-0043, Japan, and Department of Chemistry, Faculty of Engineering, Gunma University, Kiryu, Gunma 376-8515, Japan

Received December 10, 2003

The reaction of [Ni{Co(aet)₂(pyt)}₂]²⁺ (aet = 2-aminoethanethiolate, pyt = 2-pyridinethiolate) with [PtCl₄]²⁻ gave an S-bridged Co^{III}Pt^{II}Co^{III} trinuclear complex composed of two [Co(aet)₂(pyt)] units, [Pt{Co(aet)₂(pyt)}₂]²⁺ (**[1]**²⁺). When a 1:1 mixture of [Ni{Co(aet)₂(pyt)}₂]²⁺ and [Ni{Co(aet)₂(en)}₂]⁴⁺ was reacted with [PtCl₄]²⁻, a mixed-type S-bridged Co^{III}Pt^{II}Co^{III} complex composed of one [Co(aet)₂(pyt)] and one [Co(aet)₂(en)]⁺ units, [Pt{Co(aet)₂(en)}{Co(aet)₂(pyt)}]³⁺ (**[2]**³⁺), was produced, together with **[1]**²⁺ and [Pt{Co(aet)₂(en)}₂]⁴⁺. The corresponding Co^{III}Pt^{II}Co^{III} trinuclear complexes containing pymt (2-pyrimidinethiolate), [Pt{Co(aet)₂(pymt)}₂]²⁺ (**[3]**²⁺) and [Pt{Co(aet)₂(en)}{Co(aet)₂(pymt)}]³⁺ (**[4]**³⁺), were also obtained by similar reactions, using [Ni{Co(aet)₂(pymt)}₂]²⁺ instead of [Ni{Co(aet)₂(pyt)}₂]²⁺. While [Pt{Co(aet)₂(en)}₂]⁴⁺ formed both the ΔΔ (*meso*) and ΔΔ/ΛΛ (*racemic*) forms in a ratio of ca. 1:1, the preferential formation of the ΔΔ/ΛΛ form was observed for **[1]**²⁺ (ca. ΔΛ:ΔΔ/ΛΛ = 1:3) and **[2]**³⁺ (ca. Δ_{en}Λ_{pyt}/Λ_{en}Δ_{pyt}:ΔΔ/ΛΛ = 1:2). Furthermore, **[3]**²⁺ and **[4]**³⁺ predominantly formed the ΔΔ/ΛΛ form. These results indicate that the homochiral selectivity for the S-bridged Co^{III}Pt^{II}Co^{III} trinuclear complexes composed of two octahedral [Co(aet)₂(L)]⁰ or ⁺ units is enhanced in the order L = en < pyt < pymt. The isomers produced were separated and optically resolved, and the crystal structures of the *meso*-type ΔΛ-[**1**]Cl₂·4H₂O and the spontaneously resolved ΔΔ-[**4**](ClO₄)₃·H₂O were determined by X-ray analyses. In ΔΛ-[**1**]²⁺, the Δ and Λ configurational *mer*(S)·*trans*(N_{aet})-[Co(aet)₂(pyt)] units are linked by a square-planar Pt^{II} ion through four aet S atoms to form a linear-type S-bridged trinuclear structure. In ΔΔ-[**4**]³⁺, a similar linear-type trinuclear structure is constructed from the Δ-*mer*(S)·*trans*(N_{aet})-[Co(aet)₂(pymt)] and Δ-C₂-*cis*(S)-[Co(aet)₂(en)]⁺ units that are bound by a Pt^{II} ion with a slightly distorted square-planar geometry through four aet S atoms.

Introduction

Since the establishment of Werner's coordination theory by his pioneering research on the optical resolution of chiral cobalt(III) complexes,¹ chirality has been one of the most important and fascinating subject in coordination chemistry. During the past decade, much attention has been drawn to this subject in the field of coordination stereochemistry, associated with the growing interest in the design and creation of well-organized polynuclear and metallo-supramolecular species, the overall structures of which can be controlled by

chirality of their building units.^{2–3} Our research interest has been directed toward this subject, based on tris(chelate)-type cobalt(III) complexes with simple aminothiolate ligands such as 2-aminoethanethiolate (aet) and L-cysteinate (L-cys), which are linked by transition metal ions to form a variety of S-bridged polynuclear and polymeric structures.^{4–7}

* Authors to whom correspondence should be addressed. E-mail: hirotsu@chem.gunma-u.ac.jp (M.H.); konno@ch.wani.osaka-u.ac.jp (T.K.).

[†] Gunma University.

[‡] Osaka University.

(1) (a) Werner, A. *Ber. Dtsch. Chem. Ges.* **1911**, *44*, 1887. (b) Werner, A. *Ber. Dtsch. Chem. Ges.* **1912**, *45*, 121.

(2) (a) Olenyuk, B.; Fechtenkötter, A.; Stang, P. J. *J. Chem. Soc., Dalton Trans.* **1998**, 1707–1728. (b) Caulder, D. L.; Raymond, K. N. *J. Chem. Soc., Dalton Trans.* **1999**, 1185–1200. (c) Leininger, S.; Olenyuk, B.; Stang, P. J. *J. Chem. Rev.* **2000**, *100*, 853–908. (d) Swiegers, G. F.; Malefets, T. *J. Chem. Rev.* **2000**, *100*, 3483–3538.

(3) (a) Fletcher, N. C.; Keene, F. R.; Viebrock, H.; von Zelewsky, A. *Inorg. Chem.* **1997**, *36*, 1113–1121. (b) Bark, T.; Düggeli, M.; Stoeckli-Evans, H.; von Zelewsky, A. *Angew. Chem., Int. Ed.* **2001**, *40*, 2848–2851. (c) Donnelly, P. S.; Harrowfield, J. M.; Skelton, B. W.; White, A. H. *J. Chem. Soc., Dalton Trans.* **2001**, 3078–3083. (d) Katsuki, I.; Motoda, Y.; Sunatsuki, Y.; Matsumoto, N.; Nakashima, T.; Kojima, M. *J. Am. Chem. Soc.* **2002**, *124*, 629–640.

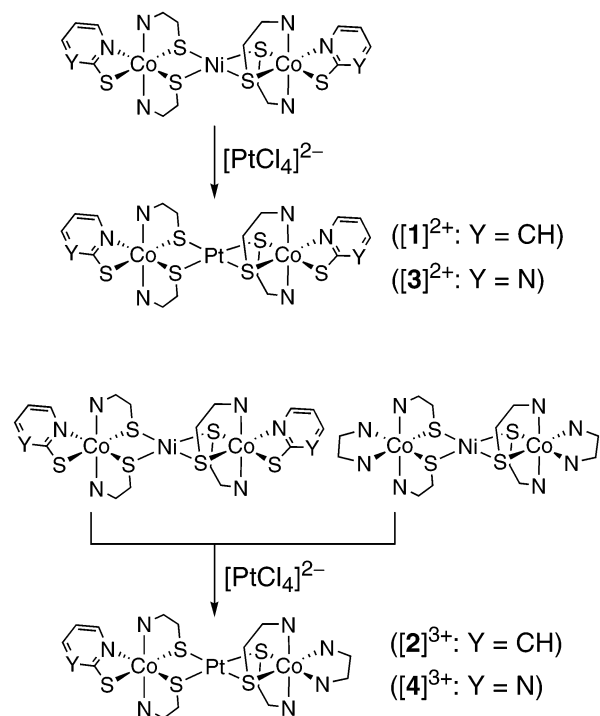
The most basic S-bridged structure of this class involves linear-type trinuclear complexes, $[M\{\text{Co}(\text{aet})_2(\text{en})\}_2]^{4+}$, in which two octahedral *cis*(S)-[Co(aet)₂(en)]⁺ units are linked by a square-planar metal ion. Previously, we have found that for M = Ni^{II} and Pd^{II} the two *cis*(S)-[Co(aet)₂(en)]⁺ units are regulated to have the same chiral configuration (Δ or Λ) to give only the *racemic* ($\Delta\Delta/\Lambda\Lambda$) form.⁵ This is in contrast to the fact that the related linear-type trinuclear complexes composed of two *fac*(S)-[Co(aet)₃] units, $[M\{\text{Co}(\text{aet})_3\}_2]^{3+}$ (M = Co^{III}, Fe^{III}), afford both the *meso* ($\Delta\Lambda$) and *racemic* ($\Delta\Delta/\Lambda\Lambda$) forms.⁶ On the other hand, recent our study has shown that linkage of the two *cis*(S)-[Co(aet)₂(en)]⁺ units by M = Pt^{II} results in the formation of the *meso* form, besides racemic one, which has been ascribed to the robustness of the Pt–S bonds.⁷ To find key factors to control the chirality of octahedral complex units aggregated in polynuclear structures, we further investigated the S-bridged Co^{III}Pt^{II}Co^{III} trinuclear system, introducing aromatic thiolate ligand pyt (2-pyridinethiolate) or pymt (2-pyrimidinethiolate) in place of en in *cis*(S)-[Co(aet)₂(en)]⁺. As a result, we found that the replacement of en in *cis*(S)-[Co(aet)₂(en)]⁺ by pyt or pymt exerts a significant effect on the chiral behavior of the Co^{III}Pt^{II}Co^{III} trinuclear complexes, although pyt or pymt does not participate in the formation of S-bridged structures with Pt^{II}. In this paper, we report on the characterization and stereochemical properties of the isomers for $[\text{Pt}\{\text{Co}(\text{aet})_2(\text{pyt})\}_2]^{2+}$ (**[1]**²⁺), $[\text{Pt}\{\text{Co}(\text{aet})_2(\text{en})\}\{\text{Co}(\text{aet})_2(\text{pyt})\}]^{3+}$ (**[2]**³⁺), $[\text{Pt}\{\text{Co}(\text{aet})_2(\text{pymt})\}_2]^{2+}$ (**[3]**²⁺), and $[\text{Pt}\{\text{Co}(\text{aet})_2(\text{en})\}\{\text{Co}(\text{aet})_2(\text{pymt})\}]^{3+}$ (**[4]**³⁺), which were newly prepared by using $[\text{Ni}\{\text{Co}(\text{aet})_2(\text{pyt})\}_2]^{2+}$, $[\text{Ni}\{\text{Co}(\text{aet})_2(\text{pymt})\}_2]^{2+}$, and $[\text{Ni}\{\text{Co}(\text{aet})_2(\text{en})\}_2]^{4+}$ as the starting materials (Scheme 1). The crystal structures of $\Delta\Lambda$ -**[1]**²⁺ and $\Delta\Delta$ -**[4]**³⁺ are also reported.

Experimental Section

All chemicals were purchased as reagent grade and used without further purification. The electronic absorption spectra were recorded with a JASCO Ubest-55 or V-530 spectrophotometer, and the CD spectra with a JASCO J-700 spectropolarimeter at room temperature. The ¹³C NMR spectra were recorded with a JEOL JNM-A500 NMR spectrometer at probe temperature in D₂O. Sodium 2,2-dimethyl-2-silapentane-5-sulfonate (DSS) was used as the internal reference. The elemental analyses (C, H, N) were performed at Osaka University. The concentrations of Co and Pt in the complexes were determined by plasma emission spectral analyses with a SHIMADZU ICP-1000III ICP spectrometer.

- (4) (a) Konno, T.; Aizawa, S.; Okamoto, K.; Hidaka, J. *Chem. Lett.* **1985**, 1017–1020. (b) Konno, T.; Nagashio, T.; Okamoto, K.; Hidaka, J. *Inorg. Chem.* **1992**, *31*, 1160–1165. (c) Konno, T.; Tokuda, K.; Suzuki, T.; Okamoto, K. *Bull. Chem. Soc. Jpn.* **1998**, *71*, 1049–1054. (d) Konno, T.; Chikamoto, Y.; Okamoto, K.; Yamaguchi, T.; Ito, T.; Hirotsu, M. *Angew. Chem., Int. Ed.* **2000**, *39*, 4098–4101. (e) Konno, T.; Yoshimura, T.; Aoki, K.; Okamoto, K.; Hirotsu, M. *Angew. Chem., Int. Ed.* **2001**, *40*, 1765–1768.
- (5) (a) Konno, T.; Okamoto, K.; Hidaka, J. *Inorg. Chem.* **1992**, *31*, 160–161. (b) Konno, T.; Hidaka, J.; Okamoto, K. *Bull. Chem. Soc. Jpn.* **1995**, *68*, 1353–1359. (c) Konno, T.; Machida, T.; Okamoto, K. *Bull. Chem. Soc. Jpn.* **1998**, *71*, 175–181.
- (6) (a) Busch, D. H.; Jicha, D. C. *Inorg. Chem.* **1962**, *1*, 884–887. (b) Brubaker, G. R.; Douglas, B. E. *Inorg. Chem.* **1967**, *6*, 1562–1566. (c) DeSimone, R. E.; Ontko, T.; Wardman, L.; Blinn, E. L. *Inorg. Chem.* **1975**, *14*, 1313–1316.
- (7) Honda, H.; Yoshimura, T.; Hirotsu, M.; Kawamoto, T.; Konno, T. *Inorg. Chem.* **2002**, *41*, 2229–2237.

Scheme 1



Caution! Perchlorate salts of metal complexes are potentially explosive and should be handled in small quantities.

Preparation, Separation, and Resolution of Complexes. **[Pt{Co(aet)₂(pyt)₂}]²⁺ (**[1]**²⁺).** To a solution containing 0.26 g (0.29 mmol) of $[\text{Ni}\{\text{Co}(\text{aet})_2(\text{pyt})\}_2]\text{Cl}_2 \cdot 7\text{H}_2\text{O}$ in 30 cm³ of water was added 0.12 g (0.29 mmol) of $\text{K}_2[\text{PtCl}_4]$ in 10 cm³ of water. The mixture was stirred at 60 °C for 1.5 h, during which time the solution color turned from dark brown to dark green. The reaction solution was filtered and poured onto an SP-Sephadex C-25 column (Na⁺ form, 4 cm × 90 cm). After the column had been washed with water, two green bands containing **[1a]**²⁺ ($\Delta\Delta/\Lambda\Lambda$ -**[1]**²⁺) and **[1b]**²⁺ ($\Delta\Lambda$ -**[1]**²⁺) were eluted in this order with a 0.15 mol dm⁻³ aqueous solution of NaCl. The **[1a]**²⁺ band was almost separated into two bands at the end of the column, and it was found from the CD spectral measurements that the earlier and the later moving bands contained the (–)₃₄₀^{CD} and (+)₃₄₀^{CD} isomers, respectively, which show CD curves enantiomeric to each other. The formation ratio of **[1b]**²⁺:**[1a]**²⁺ for this reaction was calculated to be ca. 1:3, based on the volume and absorbance of each eluate. Each eluate of the two bands was concentrated to a small volume with a rotary evaporator and then stood in a refrigerator for 3 days. The resulting green powder was collected by filtration and washed with 80% acetone and then acetone. Yield for **[1a]**Cl₂·8H₂O: 0.09 g. Anal. Calcd for $[\text{Pt}\{\text{Co}(\text{aet})_2(\text{pyt})\}_2]\text{Cl}_2 \cdot 8\text{H}_2\text{O}$, C₁₈H₄₈Cl₂Co₂N₆O₈PtS₆: C, 20.53; H, 4.60; N, 7.98; Co, 11.2; Pt, 18.5. Found: C, 20.42; H, 4.30; N, 8.04; Co, 11.5; Pt, 19.0. Yield for **[1b]**Cl₂·7H₂O: 0.02 g. Anal. Calcd for $[\text{Pt}\{\text{Co}(\text{aet})_2(\text{pyt})\}_2]\text{Cl}_2 \cdot 7\text{H}_2\text{O}$, C₁₈H₄₆Cl₂Co₂N₆O₇PtS₆: C, 20.89; H, 4.48; N, 8.12. Found: C, 20.77; H, 4.17; N, 8.19. Single crystals of **[1b]**Cl₂·4H₂O suitable for X-ray analysis were obtained by concentrating the **[1b]**²⁺ eluate to an appropriate volume, followed by storing in a refrigerator.

Complete optical resolution of **[1a]**²⁺ was performed by the column chromatographic method. An aqueous solution of **[1a]**²⁺ was chromatographed on an SP-Sephadex C-25 column (Na⁺ form,

- (8) Hirotsu, M.; Endo, R.; Yoshimura, T.; Konno, T. *Bull. Chem. Soc. Jpn.* **2003**, *76*, 1215–1221.

3.2 cm × 42 cm), using a 0.075 mol dm⁻³ aqueous solution of Na₂[Sb₂(*R,R*-tartrato)₂]·5H₂O as an eluent. When the developed band was separated into two bands in the column, the eluent was changed to a 0.3 mol dm⁻³ aqueous solution of NaBr. It was found from the CD spectral measurements that the earlier and the later moving bands contained the (-)₃₄₀^{CD} and (+)₃₄₀^{CD} isomers, respectively, which show CD spectra enantiomeric to each other. The (-)₃₄₀^{CD} eluate was concentrated to a small volume with a rotary evaporator, and the resulting green powder was collected by filtration, washed with cold water, and air-dried. Yield: 0.01 g. Anal. Calcd for [Pt{Co(aet)₂(pyt)}₂]Br₂·7H₂O, C₁₈H₄₆Br₂Co₂N₆O₇PtS₆: C, 19.24; H, 4.13; N, 7.48. Found for (-)₃₄₀^{CD}[**1a**]Br₂·7H₂O: C, 19.11; H, 4.01; N, 7.52.

[Pt{Co(aet)₂(en)}]{Co(aet)₂(pyt)}³⁺ (**[2]³⁺**). To a solution containing 0.16 g (0.18 mmol) of [Ni{Co(aet)₂(pyt)}₂]Cl₂·7H₂O⁸ and 0.15 g (0.18 mmol) of [Ni{Co(aet)₂(en)}₂]Cl₄·6H₂O^{5b} in 40 cm³ of water was added a solution containing 0.15 g (0.36 mmol) of K₂[PtCl₄] in 10 cm³ of water. The mixture was stirred at 60 °C for 1.5 h. The resulting dark brown solution was poured onto an SP-Sephadex C-25 column (Na⁺ form, 4 cm × 90 cm). After the column had been washed with water, two green bands containing [**1a**]²⁺ (ΔΔ/ΛΛ-[**1**]²⁺) and [**1b**]²⁺ (ΔΛ-[**1**]²⁺) were eluted in this order with a 0.15 mol dm⁻³ aqueous solution of NaCl, and then two brown bands containing [**2a**]³⁺ (ΔΔ/ΛΛ-[**2**]³⁺) and [**2b**]³⁺ (Δ_{en}Λ_{pyt}/Λ_{en}Δ_{pyt}-[**2**]³⁺) were eluted in this order with a 0.3 mol dm⁻³ aqueous solution of NaCl. Finally, two red-brown bands containing ΔΔ/ΛΛ-[Pt{Co(aet)₂(en)}₂]⁴⁺ and ΔΛ-[Pt{Co(aet)₂(en)}₂]⁴⁺ were eluted in this order with a 0.5 mol dm⁻³ aqueous solution of NaCl. Each of the [**2a**]³⁺ and [**2b**]³⁺ bands, as well as the [**1a**]²⁺ band, was broadened at the end of the column. It was found from the CD spectral measurements that the earlier and the later fractions of each band contained the (-)₃₄₀^{CD} and (+)₃₄₀^{CD} isomers, respectively, which show CD curves enantiomeric to each other. The formation ratio of [**2b**]³⁺: [**2a**]³⁺ for this reaction was calculated to be ca. 1:2, based on the volume and absorbance of each eluate. Each of the [**2a**]³⁺ and [**2b**]³⁺ eluates was concentrated with a rotary evaporator to deposit a dark brown powder, which was recrystallized from water by adding an appropriate amount of NaClO₄. The resulting brown powder of [**2a**](ClO₄)₃·H₂O or [**2b**](ClO₄)₃·H₂O was collected by filtration and washed with ethanol. Yield for [**2a**](ClO₄)₃·H₂O: 0.06 g. Anal. Calcd for [Pt{Co(aet)₂(en)}{Co(aet)₂(pyt)}](ClO₄)₃·H₂O, C₁₅H₃₈Cl₃Co₂N₇O₁₃PtS₅: C, 16.32; H, 3.47; N, 8.88; Co, 10.7; Pt, 17.7. Found: C, 16.21; H, 3.36; N, 8.82; Co, 10.9; Pt, 17.8. Yield for [**2b**](ClO₄)₃·H₂O: 0.02 g. Anal. Calcd for [Pt{Co(aet)₂(en)}]{Co(aet)₂(pyt)}(ClO₄)₃·H₂O, C₁₅H₃₈Cl₃Co₂N₇O₁₃PtS₅: C, 16.32; H, 3.47; N, 8.88. Found: C, 16.25; H, 3.38; N, 8.86.

[Pt{Co(aet)₂(pymt)}₂]²⁺ (**[3]²⁺**). To a solution containing 0.22 g (0.24 mmol) of [Ni{Co(aet)₂(pymt)}₂]Cl₂·8H₂O⁸ in 30 cm³ of water was added 0.10 g (0.24 mmol) of K₂[PtCl₄] in 10 cm³ of water. The mixture was stirred at 60 °C for 1.5 h, during which time the solution color turned from brown to dark green. The reaction solution was poured onto an SP-Sephadex C-25 column (Na⁺ form, 4 cm × 90 cm). After the column had been washed with water, a major dark green band containing [**3a**]²⁺ (ΔΔ/ΛΛ-[**3**]²⁺), followed by a minor pale green band containing [**3b**]²⁺ (ΔΛ-[**3**]²⁺), was eluted with a 0.15 mol dm⁻³ aqueous solution of NaCl. The formation ratio of [**3b**]²⁺: [**3a**]²⁺ for this reaction was estimated to be less than 1:10, based on the volume and absorbance of each eluate. The [**3a**]²⁺ eluate was concentrated to a small volume with a rotary evaporator to deposit a green powder containing [**3a**]Cl₂. This powder was dissolved in a small amount of water, and was poured onto an SP-Sephadex C-25 column (Na⁺ form, 4 cm × 42

cm). After the column had been washed with water, two green bands were eluted with a 0.075 mol dm⁻³ aqueous solution of Na₂[Sb₂(*R,R*-tartrato)₂]·5H₂O as an eluent. When the developed band was completely separated into two bands in the column, the eluent was changed to a 0.3 mol dm⁻³ aqueous solution of NaBr. It was found from the CD spectral measurements that the earlier and the later moving bands contained the (-)₃₄₀^{CD} and (+)₃₄₀^{CD} isomers, respectively, which show CD curves enantiomeric to each other. The (-)₃₄₀^{CD} eluate was concentrated to a small volume with a rotary evaporator, and the resulting green powder was collected by filtration, washed with cold water, and air-dried. Yield: 0.06 g. Anal. Calcd for [Pt{Co(aet)₂(pymt)}₂]Br₂·8H₂O, C₁₆H₄₆Br₂Co₂N₈O₈PtS₆: C, 16.80; H, 4.05; N, 9.80; Co, 10.3; Pt, 17.1. Found for (-)₃₄₀^{CD}[**3a**]Br₂·8H₂O: C, 16.68; H, 3.97; N, 9.80; Co, 10.3; Pt, 16.9.

Attempts to isolate [**3b**]²⁺ as a solid from the eluate were unsuccessful because of the coexistence of large quantities of NaBr relative to the complex.

[Pt{Co(aet)₂(en)}]{Co(aet)₂(pymt)}³⁺ (**[4]³⁺**). To a solution containing 0.11 g (0.12 mmol) of [Ni{Co(aet)₂(pymt)}₂]Cl₂·8H₂O⁸ and 0.10 g (0.12 mmol) of [Ni{Co(aet)₂(en)}₂]Cl₄·6H₂O^{5b} in 40 cm³ of water was added a solution containing 0.10 g (0.24 mmol) of K₂[PtCl₄] in 10 cm³ of water. The mixture was stirred at 60 °C for 1.5 h. After filtration, the dark brown solution was poured onto an SP-Sephadex C-25 column (Na⁺ form, 4 cm × 90 cm). After the column had been washed with water, two green bands of [**3a**]²⁺ (ΔΔ/ΛΛ-[**3**]²⁺) and [**3b**]²⁺ (ΔΛ-[**3**]²⁺) were eluted with a 0.15 mol dm⁻³ aqueous solution of NaCl, and then a dark brown band containing [**4a**]³⁺ (ΔΔ/ΛΛ-[**4**]³⁺), tailed by a pale brown band containing [**4b**]³⁺ (Δ_{en}Λ_{pymt}/Λ_{en}Δ_{pymt}-[**4**]³⁺), was eluted with a 0.3 mol dm⁻³ aqueous solution of NaCl. Finally, two red-brown bands containing ΔΔ/ΛΛ-[Pt{Co(aet)₂(en)}₂]⁴⁺ and ΔΛ-[Pt{Co(aet)₂(en)}₂]⁴⁺ were eluted in this order with a 0.5 mol dm⁻³ aqueous solution of NaCl. The formation ratio of [**4b**]³⁺: [**4a**]³⁺ for this reaction was estimated to be less than 1:10, based on the volume and absorbance of each eluate. The [**4a**]³⁺ eluate was concentrated to deposit a dark brown powder, which was recrystallized from water by adding an appropriate amount of NaClO₄. The resulting dark brown needle crystals were collected by filtration and washed with ethanol. Yield: 0.07 g. Anal. Calcd for [Pt{Co(aet)₂(en)}{Co(aet)₂(pymt)}](ClO₄)₃·H₂O, C₁₄H₃₇Cl₃Co₂N₈O₁₃PtS₅: C, 15.22; H, 3.37; N, 10.14; Co, 10.7; Pt, 17.7. Found: C, 15.13; H, 3.21; N, 10.10; Co, 10.6; Pt, 17.4. Single crystals of [**4a**](ClO₄)₃·H₂O suitable for X-ray analysis, which were spontaneously resolved, were obtained by recrystallization of the needle crystals from water at room temperature. Attempts to isolate [**4b**]³⁺ as a solid from the eluate were unsuccessful because of the coexistence of large quantities of NaClO₄ relative to the complex.

X-ray Structure Determination. Single-crystal X-ray diffraction experiments for ΔΛ-[**1**]Cl₂·4H₂O ([**1b**]Cl₂·4H₂O) and ΔΔ-[**4**](ClO₄)₃·H₂O ((+)₃₄₀^{CD}-[**4**](ClO₄)₃·H₂O) were performed on a Rigaku AFC-7S diffractometer with graphite-monochromatized Mo Kα radiation (λ = 0.710 69 Å). Crystallographic data are summarized in Table 1. Unit cell parameters were determined by a least-squares refinement, using the setting angles of 25 reflections (28° < 2θ < 30°). The intensity data were collected by the ω-2θ scan technique (2θ < 55°). During the data collections, the intensities of three standard reflections were measured after every 150 reflections. No significant reduction was observed for ΔΔ-[**4**](ClO₄)₃·H₂O, while the standards for ΔΛ-[**1**]Cl₂·4H₂O decreased by 10.4%. Thus, a linear correction factor was applied to the data of ΔΛ-[**1**]Cl₂·4H₂O. The intensities were corrected for Lorentz and polarization effects. Empirical absorption corrections based on a series of ψ scans were

Table 1. Crystallographic Data for $\Delta\Delta$ -[**1**]Cl₂·4H₂O and $\Delta\Delta$ -[**4**](ClO₄)₃·H₂O

	$\Delta\Delta$ -[1]Cl ₂ ·4H ₂ O	$\Delta\Delta$ -[4](ClO ₄) ₃ ·H ₂ O
empirical formula	C ₁₈ H ₄₀ Cl ₂ Co ₂ N ₆ PtS ₆ O ₄	C ₁₄ H ₃₇ Cl ₃ Co ₂ N ₈ PtS ₅ O ₁₃
fw	980.79	1105.12
cryst system	monoclinic	orthorhombic
space group	<i>P</i> 2 ₁ / <i>c</i> (No. 14)	<i>P</i> 2 ₁ 2 ₁ 2 ₁ (No. 19)
<i>a</i> , Å	7.200(2)	14.963(2)
<i>b</i> , Å	9.754(2)	16.662(2)
<i>c</i> , Å	14.529(2)	13.979(1)
β , deg	92.05(1)	
<i>V</i> , Å ³	1659.1(5)	3485.3(6)
<i>Z</i>	2	4
<i>T</i> , K	295	293
ρ_{calc} , g cm ⁻³	1.963	2.106
μ (Mo K α), mm ⁻¹	5.75	5.53
<i>R</i> ^a	0.036	0.038
<i>R</i> _w ^b	0.030	0.028

$$^a R = \sum(|F_o| - |F_c|) / \sum(|F_o|). \quad ^b R_w = [\sum w(|F_o| - |F_c|)^2 / \sum w(|F_o|)^2]^{1/2}, w = 1/\sigma^2(F_o).$$

also applied. The 2787 and 3706 independent reflections with $I > 2\sigma(I)$ of the measured 4106 and 4478 reflections were considered as “observed” and used for the structure determination of $\Delta\Delta$ -[**1**]Cl₂·4H₂O and $\Delta\Delta$ -[**4**](ClO₄)₃·H₂O, respectively. The positions of Pt, S, and some other atoms were determined by direct methods. The remaining non-H atom positions were found by successive difference Fourier techniques. The structures were refined by full-matrix least-squares techniques using anisotropic thermal parameters for non-H atoms. For $\Delta\Delta$ -[**1**]Cl₂·4H₂O, H atoms of aet were found from difference Fourier maps and refined using isotropic thermal parameters, while those of pyt were not included for the model because of its disordered structure. All H atoms for $\Delta\Delta$ -[**4**](ClO₄)₃·H₂O were located and added to calculations but not refined. All calculations were performed using the teXsan crystallographic software package.⁹

Results and Discussion

Synthesis and Characterization of [Pt{Co(aet)₂(pyt)}₂]²⁺ ([1**]²⁺).** Treatment of a dark brown solution of [Ni{Co(aet)₂(pyt)}₂]²⁺ with 1 molar equiv of [PtCl₄]²⁻ gave a dark green reaction solution, from which [**1a**]²⁺ and [**1b**]²⁺ were isolated as the chloride salts after the chromatographic separation with use of an SP-Sephadex C-25 column. The plasma emission spectral analyses indicated that each complex isolated as the chloride salt contains Co and Pt atoms in a 2:1 ratio, and their elemental analyses are consistent with the proposed formula for [Pt{Co(aet)₂(pyt)}₂]Cl₂. The crystal structure of [**1b**]²⁺, determined by X-ray analysis, demonstrated the linear-type S-bridged trinuclear structure in [Pt{Co(aet)₂(pyt)}₂]²⁺ that is composed of two [Co(aet)₂(pyt)] units with a *mer(S)·trans(N_{aet})* configuration (vide infra). Considering the chiral configurations (Δ and Λ) of each *mer(S)·trans(N_{aet})*-[Co(aet)₂(pyt)] unit, three isomers ($\Delta\Delta$, $\Lambda\Lambda$, and $\Delta\Lambda$) are possible for [Pt{Co(aet)₂(pyt)}₂]²⁺, where Δ or Λ designate the chirality due to the skew pair of three chelate rings around each Co^{III} center.¹⁰ X-ray analysis indicated the $\Delta\Delta$ (*meso*) form for [**1b**]²⁺, which is compatible with the fact that [**1b**]²⁺ was not optically resolved. As shown in Figure 1 and Table 2, the electronic absorption spectrum of [**1a**]²⁺ in water is

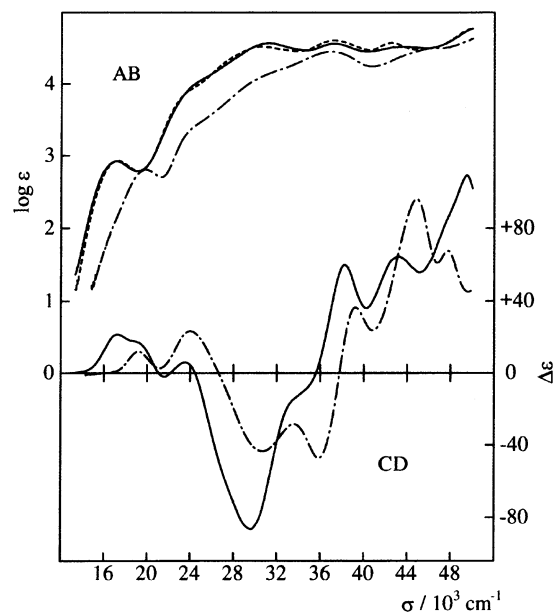


Figure 1. Electronic absorption and CD spectra of (—)^{CD}₃₄₀[**1a**]²⁺ ($\Delta\Delta$ -[**1**]²⁺) (---), [**1b**]²⁺ ($\Delta\Delta$ -[**1**]²⁺) (---), and $\Lambda\Lambda$ -[Pt{Co(aet)₂(en)}₂]⁴⁺ (- · -) in water.

very similar to that of [**1b**]²⁺ over the whole region. In particular, [**1a**]²⁺ and [**1b**]²⁺ exhibit almost overlapping visible bands at ca. $17 \times 10^3 \text{ cm}^{-1}$, which seems to be assignable as arising from a d–d transition for the terminal Co^{III} centers.^{4,7} Since [**1a**]²⁺ was optically resolved into the (–)^{CD}₃₄₀ and (+)^{CD}₃₄₀ isomers, which show CD spectra enantiomeric to each other, this complex is assigned to have the $\Delta\Delta/\Lambda\Lambda$ (*racemic*) form of [Pt{Co(aet)₂(pyt)}₂]²⁺. It is interesting to note that [**1a**]²⁺ was almost separated into two bands of its enantiomers, (–)^{CD}₃₄₀ and (+)^{CD}₃₄₀, in the SP-Sephadex C-25 column, even when the adsorbed band was eluted with an aqueous solution of NaCl. Because the resin of SP-Sephadex comprising D-glucose is chiral,¹¹ this is not to be unexpected but is quite rare, with examples of optical resolution made by the use of an achiral eluting agent being limited to a few mononuclear chromium(III) complexes.¹² The overall CD spectral pattern of (–)^{CD}₃₄₀-[**1a**]²⁺ is comparable with that of the $\Lambda\Lambda$ isomer of [Pt{Co(aet)₂(en)}₂]²⁺ (Figure 1), in which two Λ configurational *C*₂-*cis(S)*-[Co(aet)₂(en)]⁺ units are linked by a Pt^{II} ion.⁷ This suggests that (–)^{CD}₃₄₀-[**1a**]²⁺ and (+)^{CD}₃₄₀-[**1a**]²⁺ have the $\Lambda\Lambda$ and $\Delta\Delta$ configurations, respectively.

In the ¹³C NMR spectrum in D₂O, each of $\Delta\Delta/\Lambda\Lambda$ -[**1**]²⁺ ([**1a**]²⁺) and $\Delta\Delta$ -[**1**]²⁺ ([**1b**]²⁺) shows five pyt aromatic carbon signals at a lower magnetic field (δ 120–180) and

- (10) Each Co^{III}Pt^{II}Co^{III} trinuclear complex also possesses the conformational chirality (δ or λ) due to the aet chelate rings. In this paper only the configurational chirality is dealt with, because of its dominant contribution to CD spectra and of the rapid inversion of the chelate ring conformation in solution.
- (11) Yoshikawa, Y.; Yamasaki, K. *Coord. Chem. Rev.* **1979**, *28*, 205–229.
- (12) (a) Kanno, H.; Utsuno, S.; Fujita, J. *Bull. Chem. Soc. Jpn.* **1986**, *59*, 1293–1295. (b) Kanno, H.; Yamamoto, J.; Murahashi, S.; Utsuno, S.; Fujita, J. *Bull. Chem. Soc. Jpn.* **1991**, *64*, 2936–2941. (c) Kanno, H.; Yamamoto, J.; Utsuno, S.; Fujita, J. *Bull. Chem. Soc. Jpn.* **1996**, *69*, 665–671.

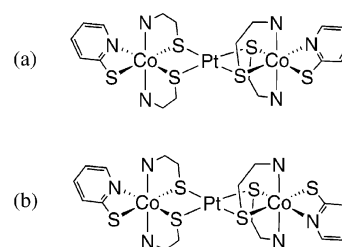
(9) *Crystal Structure Analysis Package*; Molecular Structure Corp.: Woodlands, TX, 1985 and 1992.

Table 2. Absorption and CD Spectral Data for $\Delta\Delta$ -[1]²⁺, $\Delta\Delta$ -[1]²⁺, $\Delta\Delta$ -[2]³⁺, $\Delta_{en}\Lambda_{pyr}$ -[2]³⁺, $\Lambda\Lambda$ -[3]²⁺, and $\Delta\Delta/\Lambda\Lambda$ -[4]³⁺ in H₂O^a

abs max: $\sigma/10^3 \text{ cm}^{-1}$	log ϵ for abs max/mol ⁻¹ dm ³ cm ⁻¹	CD extrema: $\sigma/10^3 \text{ cm}^{-1}$	$\Delta\epsilon$ for CD extrema/mol ⁻¹ dm ³ cm ⁻¹
$\Lambda\Lambda$ -[Pt{Co(aet) ₂ (pyt)}] ₂ ²⁺ ((-) ^{CD} ₃₄₀ -[2b] ³⁺)			
17.11	2.92	17.24	+21.5
25.1	4.07 ^{sh}	21.57	-2.0
31.13	4.57	23.50	+6.0
37.17	4.56	29.63	-86.3
43.63	4.52	38.17	+60.1
		43.10	+64.6
$\Delta\Delta$ -[Pt{Co(aet) ₂ (pyt)}] ₂ ²⁺ ([1b] ²⁺)			
17.24	2.93		
24.3	3.95 ^{sh}		
30.53	4.52		
37.20	4.61		
42.48	4.57		
$\Lambda\Lambda$ -[Pt{Co(aet) ₂ (en)}]{Co(aet) ₂ (pyt)}] ₂ ³⁺ ((-) ^{CD} ₃₄₀ -[2a] ³⁺)			
17.7	2.65 ^{sh}	19.10	+9.0
20.1	2.79 ^{sh}	23.72	+8.4
25.1	3.79 ^{sh}	29.94	-40.3
32.77	4.41	34.97	-15.3
37.34	4.43	38.61	+24.8
43.94	4.44	44.05	+44.5
$\Delta_{en}\Lambda_{pyr}$ -[Pt{Co(aet) ₂ (en)}]{Co(aet) ₂ (pyt)}] ₂ ³⁺ ((-) ^{CD} ₃₄₀ -[2b] ³⁺)			
17.7	2.64 ^{sh}	16.93	+5.6
20.1	2.78 ^{sh}	23.07	-7.4
24.3	3.68 ^{sh}	29.41	-16.4
31.63	4.36	35.40	-0.7
37.74	4.49	38.91	+13.6
42.92	4.49	45.05	-13.6
$\Lambda\Lambda$ -[Pt{Co(aet) ₂ (pymt)}] ₂ ²⁺ ((-) ^{CD} ₃₄₀ -[3a] ²⁺)			
17.39	2.99	17.53	+24.5
25.1	4.04 ^{sh}	29.11	-85.2
31.21	4.56	34.48	-18.2
37.74	4.50	38.68	+75.9
42.59	4.53	44.35	+63.5
$\Delta\Delta$ -[Pt{Co(aet) ₂ (en)}]{Co(aet) ₂ (pymt)}] ₂ ³⁺ ((-) ^{CD} ₃₄₀ -[4a] ³⁺)			
18.2	2.75 ^{sh}	30.16	+
24.9	3.79 ^{sh}	34.70	+
33.92	4.47	38.91	-
37.68	4.42		
43.82	4.47 ^{sh}		

^a The sh label denotes a shoulder.

four aet methylene carbon signals at a higher magnetic field (δ 35–60), which is compatible with the C₂-symmetrical structure in [Pt{Co(aet)₂(pyt)}]₂²⁺ (Table 3). However, it is noticed that each of one or two SCH₂ and one aromatic carbon signals splits into two for $\Delta\Delta/\Lambda\Lambda$ -[1]²⁺ and $\Delta\Lambda$ -[1]²⁺, indicative of the presence of two isomers. In addition to the *meso*-*racemic* ($\Delta\Delta$ - $\Delta\Delta/\Lambda\Lambda$) isomerism, another isomerism of *syn*-*anti*, which arises from the relative configuration of the two nonbridging pyt S atoms, is possible for [Pt{Co(aet)₂(pyt)}]₂²⁺ (Chart 1). Since the X-ray analysis

Chart 1

for $\Delta\Lambda$ -[1]²⁺ suggested the presence of both the *syn* and *anti* forms in crystal (vide infra), it is considered that each of $\Delta\Delta/\Lambda\Lambda$ -[1]²⁺ and $\Delta\Lambda$ -[1]²⁺ exists as a mixture of the *syn* and *anti* forms. Attempts to separate the *syn* and *anti* forms for each of $\Delta\Delta/\Lambda\Lambda$ -[1]²⁺ and $\Delta\Lambda$ -[1]²⁺ by SP-Sephadex C-25 column chromatography were unsuccessful, which is understood by their chemical similarities as shown by the NMR spectral behavior. The splitting of several SCH₂ and aromatic carbon signals has also been recognized for the ¹³C NMR spectra of [M{Co(aet)₂(pyt)}]₂²⁺ (M = Ni^{II}, Pd^{II}), and the presence of the *syn* and *anti* forms has been proposed to explain this NMR spectral characteristic.⁸

Synthesis and Characterization of [Pt{Co(aet)₂(en)}]{Co(aet)₂(pyt)}]₂³⁺ ([2]³⁺). The reaction of a 1:1 mixture of [Ni{Co(aet)₂(pyt)}]₂²⁺⁸ and [Ni{Co(aet)₂(en)}]₂⁴⁺^{5b} with [PtCl₄]²⁻ in water gave a dark brown solution containing [2a]³⁺ and [2b]³⁺, besides $\Delta\Delta/\Lambda\Lambda$ - and $\Delta\Lambda$ -[1]²⁺ and $\Delta\Delta/\Lambda\Lambda$ - and $\Delta\Lambda$ -[Pt{Co(aet)₂(en)}]₂⁴⁺,⁷ which were separated by SP-Sephadex C-25 column chromatography. The plasma emission spectral and elemental analyses of [2a]³⁺ and [2b]³⁺ isolated as the perchlorate salts are in agreement with the formula for [Pt{Co(aet)₂(en)}]{Co(aet)₂(pyt)}(ClO₄)₃. In the ¹³C NMR spectrum in D₂O, each of [2a]³⁺ and [2b]³⁺ shows en methylene and pyt aromatic carbon signals, besides aet methylene carbon signals, and these signals are located at almost the same magnetic fields as the corresponding signals observed for [Pt{Co(aet)₂(en)}]₂⁴⁺⁷ and [Pt{Co(aet)₂(pyt)}]₂²⁺ ([1]²⁺) (Table 3). Moreover, the overall absorption spectral features of [2a]³⁺ and [2b]³⁺ are just between those of [Pt{Co(aet)₂(en)}]₂⁴⁺ and [1]²⁺ (Figures 1 and 2), showing a d-d transition band with two components at ca. 18 × 10³ and 20 × 10³ cm⁻¹. Accordingly, it is assigned that [2a]³⁺ and [2b]³⁺ are the isomers for a mixed-type S-bridged Co^{III}-Pt^{II}Co^{III} trinuclear complex, [Pt{Co(aet)₂(en)}]{Co(aet)₂(pyt)}]₂³⁺, in which two types of octahedral Co^{III} units, *mer*(S)·*trans*(N_{aet})-[Co(aet)₂(pyt)] and C₂-*cis*(S)-[Co(aet)₂(en)]⁺, are linked by a Pt^{II} ion.

Like $\Delta\Delta/\Lambda\Lambda$ -[1]²⁺, each of [2a]³⁺ and [2b]³⁺ was optically resolved by the SP-Sephadex C-25 column chro-

Table 3. ¹³C NMR Spectral Data for Co^{III}Pt^{II}Co^{III} Trinuclear Complexes in D₂O (Chemical Shift/ppm from DSS)

complex	CH ₂ S (aet)		CH ₂ N (en)	CH ₂ N (aet)			pyt or pymt						
[1a] ²⁺	35.67	36.88		54.69	56.21		121.50	130.47	140.65	149.65	178.23		
	35.92	37.16								149.68			
[1b] ²⁺	36.88	38.09		54.47	55.79		121.48	130.50	140.67	149.50	178.13		
		38.21							149.55				
[2a] ³⁺	35.89	36.14	36.41	37.14	46.53	54.77	54.93	56.18	121.56	130.50	140.71	149.72	178.24
[2b] ³⁺	36.99	37.20	37.29	38.29	46.50	54.45	54.61	55.80	121.53	130.53	140.71	149.53	178.17
[3a] ²⁺	35.91	37.29				54.77	56.21		118.73		159.05	161.63	185.35
	36.18	37.60									159.09		
[4a] ³⁺	36.00	36.14	36.44	37.45	46.50	54.68	54.96	56.00	118.74		159.07	161.64	185.27

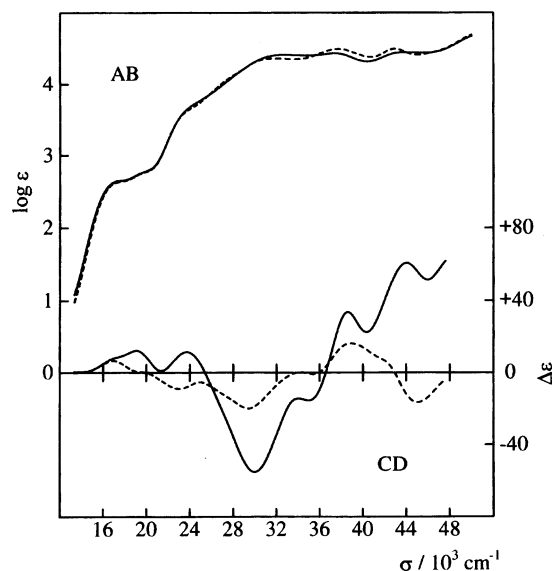


Figure 2. Electronic absorption and CD spectra of $(-)^{340\text{CD}}\text{[2a]}^{3+}$ ($\Lambda\Lambda\text{-[2]}^{3+}$) (—) and $(-)^{340\text{CD}}\text{[2b]}^{3+}$ ($\Delta_{\text{en}}\Lambda_{\text{pyt}}\text{-[2]}^{3+}$) (---) in water.

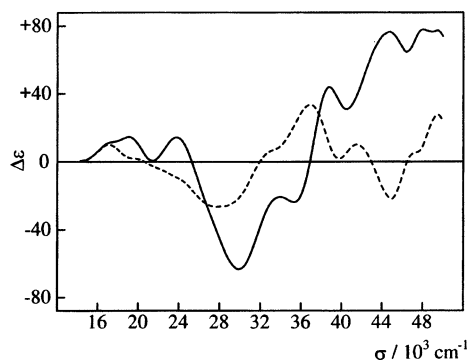


Figure 3. Calculated CD curves for $[\Delta\epsilon\{\Lambda\Lambda\text{-[Pt}\{\text{Co}(\text{aet})_2(\text{en})\}_2\}^{4+}\} + \Delta\epsilon\{\Lambda\Lambda\text{-[Pt}\{\text{Co}(\text{aet})_2(\text{pynt})\}_2\}^{2+}\}]/2$ (—) and $[\Delta\epsilon\{\Lambda\Lambda\text{-[Pt}\{\text{Co}(\text{aet})_2(\text{pynt})\}_2\}^{2+}\} - \Delta\epsilon\{\Lambda\Lambda\text{-[Pt}\{\text{Co}(\text{aet})_2(\text{en})\}_2\}^{4+}\}]/2$ (---).

matography, eluting with an aqueous solution of NaCl; the earlier and later fractions for each of the $[\mathbf{2a}]^{3+}$ and $[\mathbf{2b}]^{3+}$ eluates contained the $(-)^{340\text{CD}}$ and $(+)^{340\text{CD}}$ isomers, respectively. Since the CD spectral feature of $(-)^{340\text{CD}}\text{[2a]}^{3+}$ resembles that of $\Lambda\Lambda\text{-[Pt}\{\text{Co}(\text{aet})_2(\text{en})\}_2\}^{4+}$ (Figures 1 and 2), $(-)^{340\text{CD}}\text{[2a]}^{3+}$ is assigned to the $\Lambda\Lambda$ isomer of $[\text{Pt}\{\text{Co}(\text{aet})_2(\text{en})\}\{\text{Co}(\text{aet})_2(\text{pynt})\}]^{3+}$ ($\Lambda\Lambda\text{-[2]}^{3+}$) having $\Lambda\text{-}C_2\text{-cis}(S)\text{-[Co}(\text{aet})_2(\text{en})\]^+$ and $\Lambda\text{-mer}(S)\cdot\text{trans}(N_{\text{aet}})\text{-[Co}(\text{aet})_2(\text{pynt})\]$ units, while $(+)^{340\text{CD}}\text{[2a]}^{3+}$ that shows CD spectrum enantiomeric to $(-)^{340\text{CD}}\text{[2a]}^{3+}$ is the $\Delta\Delta$ isomer ($\Delta\Delta\text{-[2]}^{3+}$). Assuming that this assignment is correct and that the CD contributions from the two terminal Co^{III} units in the S-bridged $\text{Co}^{\text{III}}\text{Pt}^{\text{II}}\text{Co}^{\text{III}}$ trinuclear structure are additive, the CD curve calculated from the equation $[\Delta\epsilon\{\Lambda\Lambda\text{-[Pt}\{\text{Co}(\text{aet})_2(\text{en})\}_2\}^{4+}\} + \Delta\epsilon\{\Lambda\Lambda\text{-[Pt}\{\text{Co}(\text{aet})_2(\text{pynt})\}_2\}^{2+}\}]/2$ would represent the CD spectrum of $\Lambda\Lambda\text{-[Pt}\{\text{Co}(\text{aet})_2(\text{en})\}\{\text{Co}(\text{aet})_2(\text{pynt})\}]^{3+}$ ($\Lambda\Lambda\text{-[2]}^{3+}$). As shown in Figure 3, the CD curve calculated from this equation coincides well with the observed CD curve of $\Lambda\Lambda\text{-[2]}^{3+}$. This implies that the additivity on CD, which has been recognized mainly for the mononuclear Co^{III} system,¹³ is valid for the present S-bridged $\text{Co}^{\text{III}}\text{Pt}^{\text{II}}\text{Co}^{\text{III}}$ trinuclear system. While $[\mathbf{2a}]^{3+}$ ($\Delta\Delta/\Lambda\Lambda\text{-[2]}^{3+}$) and $[\mathbf{2b}]^{3+}$ exhibit absorption spectra quite similar to each

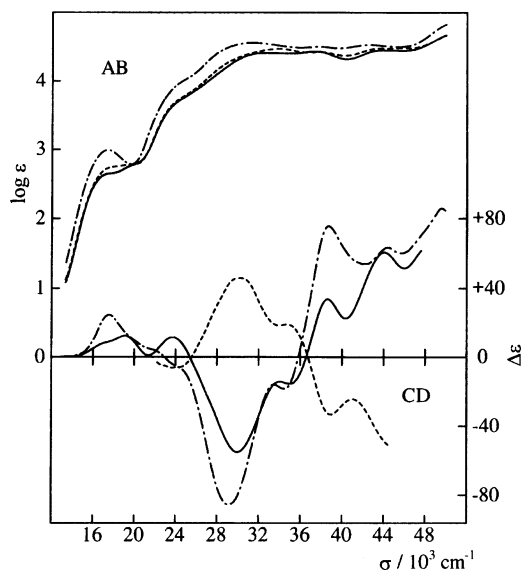


Figure 4. Electronic absorption and CD spectra of $(-)^{340\text{CD}}\text{[3a]}^{2+}$ ($\Lambda\Lambda\text{-[3]}^{2+}$) (· · ·), $(+)^{340\text{CD}}\text{[4a]}^{3+}$ ($\Delta\Delta\text{-[4]}^{3+}$) (---), and $(-)^{340\text{CD}}\text{[2a]}^{3+}$ ($\Lambda\Lambda\text{-[2]}^{3+}$) (—) in water. The CD intensity for $(+)^{340\text{CD}}\text{[4a]}^{3+}$ is arbitrary.

other, the CD spectral features of the optically resolved isomers of $[\mathbf{2b}]^{3+}$ are differ markedly from those of $\Delta\Delta\text{-}$ and $\Lambda\Lambda\text{-[2]}^{3+}$ (Figure 2), exhibiting lower CD intensities over the whole region. Figure 3 also illustrates the CD curve calculated from the equation $[\Delta\epsilon\{\Lambda\Lambda\text{-[Pt}\{\text{Co}(\text{aet})_2(\text{pynt})\}_2\}^{2+}\} - \Delta\epsilon\{\Lambda\Lambda\text{-[Pt}\{\text{Co}(\text{aet})_2(\text{en})\}_2\}^{4+}\}]/2$, which would represent the CD spectrum of the quasi-*meso*-type $\Delta_{\text{en}}\Lambda_{\text{pyt}}$ isomer of $[\text{Pt}\{\text{Co}(\text{aet})_2(\text{en})\}\{\text{Co}(\text{aet})_2(\text{pynt})\}]^{3+}$, assuming that the CD contributions from the two terminal Co^{III} units are additive. Since this calculated curve is in agreement with the observed CD curve of $(-)^{340\text{CD}}\text{[2b]}^{3+}$, it is assigned that $(-)^{340\text{CD}}\text{[2b]}^{3+}$ is $\Delta_{\text{en}}\Lambda_{\text{pyt}}\text{-[Pt}\{\text{Co}(\text{aet})_2(\text{en})\}\{\text{Co}(\text{aet})_2(\text{pynt})\}]^{3+}$ ($\Delta_{\text{en}}\Lambda_{\text{pyt}}\text{-[2]}^{3+}$) composed of $\Delta\text{-}C_2\text{-cis}(S)\text{-[Co}(\text{aet})_2(\text{en})\]^+$ and $\Lambda\text{-mer}(S)\cdot\text{trans}(N_{\text{aet}})\text{-[Co}(\text{aet})_2(\text{pynt})\]$ units, while $(+)^{340\text{CD}}\text{[2b]}^{3+}$ that shows CD spectrum enantiomeric to $(-)^{340\text{CD}}\text{[2b]}^{3+}$ is the $\Lambda_{\text{en}}\Delta_{\text{pyt}}$ isomer ($\Lambda_{\text{en}}\Delta_{\text{pyt}}\text{-[2]}^{3+}$).

Synthesis and Characterization of $[\text{Pt}\{\text{Co}(\text{aet})_2(\text{pynt})\}_2]^{2+}$ ($[\mathbf{3}]^{2+}$) and $[\text{Pt}\{\text{Co}(\text{aet})_2(\text{en})\}\{\text{Co}(\text{aet})_2(\text{pynt})\}]^{3+}$ ($[\mathbf{4}]^{3+}$). The reaction of $[\text{Ni}\{\text{Co}(\text{aet})_2(\text{pynt})\}_2]^{2+}$ ⁸ with $[\text{PtCl}_4]^{2-}$ in water gave a dark green solution containing $[\mathbf{3a}]^{2+}$ and $[\mathbf{3b}]^{2+}$, which were separated by SP-Sephadex C-25 column chromatography. The formation ratio of $[\mathbf{3b}]^{2+}$: $[\mathbf{3a}]^{2+}$ was estimated to be less than 1:10. The plasma emission spectral analyses indicated that each of the $[\mathbf{3a}]^{2+}$ and $[\mathbf{3b}]^{2+}$ eluates contains Co and Pt atoms in a 2:1 ratio. The absorption spectra of the two eluates, which are quite similar to each other, correspond well with those of $\Delta\Delta/\Lambda\Lambda\text{-}$ and $\Delta\Lambda\text{-[Pt}\{\text{Co}(\text{aet})_2(\text{pynt})\}_2\}^{2+}$ ($[\mathbf{1}]^{2+}$) (Table 2 and Figures 1 and 4). The earlier and later fractions of the $[\mathbf{3a}]^{2+}$ eluate were CD active, while no CD was recognized for each fraction of the $[\mathbf{3b}]^{2+}$ eluate. From these facts, together with the elemental analysis for $[\mathbf{3a}]\text{Br}_2$, it is reasonable to assign

(13) (a) Hawkins, C. J. *Absolute Configuration of Metal Complexes*; John Wiley & Sons Ltd.: New York, 1971. (b) Konno, T.; Okamoto, K.; Einaga, H.; Hidaka, J. *Chem. Lett.* **1983**, 969–970. (c) Konno, T.; Okamoto, K.; Einaga, H.; Hidaka, J. *Bull. Chem. Soc. Jpn.* **1985**, 58, 1119–1124.

that $[3a]^{2+}$ and $[3b]^{2+}$ are the $\Delta\Delta/\Lambda\Lambda$ and $\Delta\Lambda$ forms of $[Pt\{Co(aet)_2(pynt)\}_2]^{2+}$, respectively. Complex $\Delta\Delta/\Lambda\Lambda$ - $[3]^{2+}$ was completely resolved into the enantiomers, $(-)^{CD}_{340}$ and $(+)^{CD}_{340}$, by SP-Sephadex C-25 column chromatography, using $[Sb_2(R,R\text{-tartrato})_2]^{2-}$ as an eluent. Since the CD spectrum of $(-)^{CD}_{340}$ - $[3]^{2+}$ is quite similar to that of $\Lambda\Lambda$ - $[1]^{2+}$ over the whole region (Figures 1 and 4), $(-)^{CD}_{340}$ and $(+)^{CD}_{340}$ - $[3]^{2+}$ are assignable to the $\Lambda\Lambda$ and $\Delta\Delta$ isomers of $[Pt\{Co(aet)_2(pynt)\}_2]^{2+}$, respectively. The ^{13}C NMR spectrum of $\Delta\Delta/\Lambda\Lambda$ - $[3]^{2+}$ ($[3a]^{2+}$) in D_2O exhibits four pynt aromatic carbon signals at a lower magnetic field, besides two SCH_2 and two NH_2 aet methylene carbon signals at a higher magnetic field (Table 3), which supports the C_2 -symmetrical S-bridged $Co^{III}Pt^{II}Co^{III}$ structure in $[Pt\{Co(aet)_2(pynt)\}_2]^{2+}$. The splitting of two SCH_2 signals, besides one aromatic carbon signal, is observed for $\Delta\Delta/\Lambda\Lambda$ - $[3]^{2+}$, as in the case of $\Delta\Delta/\Lambda\Lambda$ - $[1]^{2+}$. This suggests that $\Delta\Delta/\Lambda\Lambda$ - $[3]^{2+}$ also exists as a mixture of the *syn* and *anti* forms.

The reaction of a mixture of $[Ni\{Co(aet)_2(pynt)\}_2]^{2+}$ and $[Ni\{Co(aet)_2(en)\}_2]^{4+}$ with $[PtCl_4]^{2-}$ in water produced a dark brown solution containing $[4a]^{3+}$ and $[4b]^{3+}$, besides $\Delta\Delta/\Lambda\Lambda$ - and $\Delta\Lambda$ - $[3]^{2+}$ and $\Delta\Delta/\Lambda\Lambda$ - and $\Delta\Lambda$ - $[Pt\{Co(aet)_2(en)\}_2]^{4+}$, which were separated by SP-Sephadex C-25 column chromatography. The formation ratio of $[4b]^{3+}$: $[4a]^{3+}$ in this reaction was estimated to be less than 1:10. Complex $[4a]^{3+}$ was isolated as the perchlorate salt, and its elemental and plasma emission spectral analyses were consistent with the formula for $[Pt\{Co(aet)_2(en)\}\{Co(aet)_2(pynt)\}](ClO_4)_3$. In the ^{13}C NMR spectrum in D_2O , $[4a]^{3+}$ exhibits en methylene and pynt aromatic carbon signals, besides aet methylene carbon signals (Table 3). These results indicate that $[4a]^{3+}$ has the mixed-type S-bridged $Co^{III}Pt^{II}Co^{III}$ trinuclear structure in $[Pt\{Co(aet)_2(en)\}\{Co(aet)_2(pynt)\}]^{3+}$ composed of C_2 -*cis*(S)- $[Co(aet)_2(en)]^+$ and *mer*(S)·*trans*(N_{aet})- $[Co(aet)_2(pynt)]$ units, taking account of its absorption spectrum quite similar to $[Pt\{Co(aet)_2(en)\}\{Co(aet)_2(pynt)\}]^{3+}$ ($[2]^{3+}$) over the whole region (Figures 2 and 4). Since X-ray analysis for the spontaneously resolved $(+)^{CD}_{340}$ - $[4a]^{3+}$ established the $\Delta\Delta$ configurational S-bridged structure in $[Pt\{Co(aet)_2(en)\}\{Co(aet)_2(pynt)\}]^{3+}$ (vide infra), $[4a]^{3+}$ is confidently assigned to have the *racemic* form ($\Delta\Delta/\Lambda\Lambda$ - $[4]^{3+}$). The absorption spectral feature of $[4b]^{3+}$ is essentially the same as that of $[4a]^{3+}$, suggesting that $[4b]^{3+}$ has the quasi-*meso*-type form of $[Pt\{Co(aet)_2(en)\}\{Co(aet)_2(pynt)\}]^{3+}$ ($\Delta_{en}\Lambda_{pynt}/\Lambda_{en}\Delta_{pynt}$ - $[4]^{3+}$). Figure 4 comprises the CD spectral curve of the single crystal of $\Delta\Delta$ - $[4]^{3+}$ used for X-ray analysis, together with the CD curve of $(-)^{CD}_{340}$ - $[2a]^{3+}$ that is assigned to the $\Lambda\Lambda$ isomer of $[Pt\{Co(aet)_2(en)\}\{Co(aet)_2(pynt)\}]^{3+}$ based on the CD curve analysis. Since the two curves are almost enantiomeric to each other, it is seen that this configurational assignment of $(-)^{CD}_{340}$ - $[2a]^{3+}$ is correct and that the alternation of the terminal chelating ligands in the S-bridged $Co^{III}Pt^{II}Co^{III}$ trinuclear structure does not affect CD so much.

Crystal Structure of $[1b]Cl_2\cdot 4H_2O$ ($\Delta\Lambda$ - $[1]Cl_2\cdot 4H_2O$). X-ray analysis of $[1b]Cl_2\cdot 4H_2O$ revealed the presence of a discrete complex cation, two Cl^- anions, and water molecules

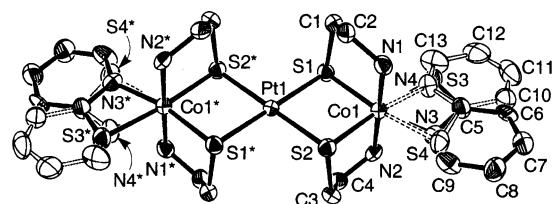
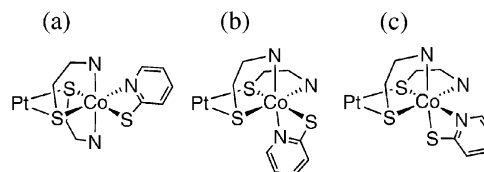


Figure 5. Perspective view of $[1b]^{2+}$ ($\Delta\Lambda$ - $[1]^{2+}$) with the atomic labeling scheme. Ellipsoids represent 50% probability. Hydrogen atoms are omitted for clarity.

Table 4. Selected Bond Distances (Å) and Angles (deg) for $\Delta\Lambda$ - $[1]Cl_2\cdot 4H_2O$

Distances			
Pt1—S1	2.327(2)	Co1—S4	2.346(8)
Pt1—S2	2.328(2)	Co1—N1	1.973(6)
Co1—S1	2.253(2)	Co1—N2	1.971(6)
Co1—S2	2.258(2)	Co1—N3	1.93(2)
Co1—S3	2.383(7)	Co1—N4	1.92(2)
Angles			
S1—Pt1—S2	84.13(6)	S3—Co1—N3	71.0(8)
S1—Co1—S2	87.46(7)	S4—Co1—N4	73.4(8)
S1—Co1—N1	87.5(2)	Pt—S1—Co1	94.28(7)
S2—Co1—N2	87.6(2)	Pt—S2—Co1	94.12(8)

Chart 2



of crystallization. The number of the Cl^- anion implies that the entire complex cation $[1b]^{2+}$ is divalent. The structure of the entire complex cation is shown in Figure 5, and its selected bond distances and angles are listed in Table 4. The complex cation $[1b]^{2+}$ consists of two approximately octahedral $[Co(aet)_2(pynt)]$ units and one Pt atom. The two aet S atoms of each $[Co(aet)_2(pynt)]$ units are bound to the central Pt atom to form a linear-type S-bridged $Co^{III}Pt^{II}Co^{III}$ trinuclear structure in $[Pt\{Co(aet)_2(pynt)\}_2]^{2+}$. The crystallographic center of inversion located at the Pt atom requires that the three metal atoms are arranged to be exactly linear with the identical Pt—Co distances (3.3579(9) Å). Three geometrical configurations (*mer*(S)·*trans*(N_{aet}), *mer*(S)·*cis*(N_{aet}), and *fac*(S)·*cis*(N_{aet})) are possible for $[Co(aet)_2(pynt)]$ that chelates to Pt atom through two aet S atoms (Chart 2). In $[1b]^{2+}$, each $[Co(aet)_2(pynt)]$ unit adopts the *mer*(S)·*trans*(N_{aet}) configuration with two aet S atoms in the equatorial positions and two aet N atoms at the apical positions. The arrangement of two aet ligands in the *mer*(S)·*trans*(N_{aet})- $[Co(aet)_2(pynt)]$ unit is the same as that in the C_2 -*cis*(S)- $[Co(aet)_2(en)]$ unit, which are commonly observed for the related S-bridged trinuclear structures in $[M\{Co(aet)_2(en)\}_2]^{4+}$ ($M = Ni^{II}, Pd^{II}, Pt^{II}$).^{5,7} The two units in $[1b]^{2+}$ have the Δ and Λ configurations to give the *meso* form, as indicated by the inversion center at the central Pt atom. It is worth to note that each pynt ligand appears to be disordered in its molecular plane. This disorder can be rationalized by coexistence of the *syn* and *anti* forms rather than the disorder of the sole complex cation with either the *syn* or *anti* form.

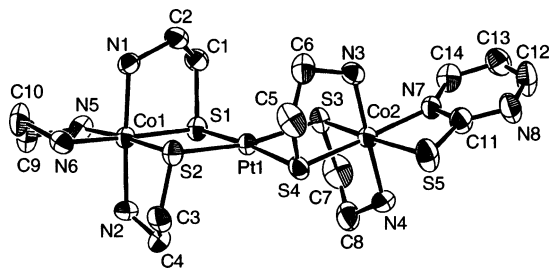


Figure 6. Perspective view of (+)₃₄₀^{CD}-[4a]³⁺ ($\Delta\Delta$ -[4]³⁺) with the atomic labeling scheme. Ellipsoids represent 50% probability. Hydrogen atoms are omitted for clarity.

The Co–S_{aet} (average 2.256(2) Å) and Co–N_{aet} (average 1.972(6) Å) bond distances in $\Delta\Delta$ -[1]²⁺ (**1b**)²⁺ are similar to the corresponding distances in $\Delta\Delta$ -[Pt{Co(aet)₂(en)}₂]⁴⁺ (average Co–S = 2.244(5) Å, Co–N = 1.98(2) Å).⁷ Furthermore, the Pt–S distances (average 2.328(2) Å) in $\Delta\Delta$ -[1]²⁺ is in agreement with those in $\Delta\Delta$ -[Pt{Co(aet)₂(en)}₂]⁴⁺ (average 2.318(5) Å). Thus, the introduction of bidentate-*N,S* pyt ligand in place of bidentate-*N,N* en ligand little affects the coordinating ability of aet S atoms not only toward the terminal Co^{III} atom but also toward the central Pt^{II} atom. On the other hand, the Co–S_{pyt} bond distances in $\Delta\Delta$ -[1]²⁺ (average 2.365(8) Å) are larger than those found in *mer*(*S*)-[Co(pyt)₃] (average 2.298(1) Å),^{14a} while the Co–N_{pyt} distances in $\Delta\Delta$ -[1]²⁺ (average 1.93(2) Å) and *mer*(*S*)-[Co(pyt)₃] (average 1.917(3) Å) are comparable to each other. This suggests that the pyt S atom in the *mer*(*S*)·*trans*(*N*_{aet})-[Co(aet)₂(pyt)] unit is weakly bound to the Co^{III} center, compared with the S atoms in *mer*(*S*)-[Co(pyt)₃], although the disordered structure of pyt in $\Delta\Delta$ -[1]²⁺ precludes the precise comparison.

Crystal Structure of (+)₃₄₀^{CD}-[4a](ClO₄)₃·H₂O ($\Delta\Delta$ -[4](ClO₄)₃·H₂O). X-ray structural analysis of (+)₃₄₀^{CD}-[4a]³⁺ showed the presence of a discrete complex cation, three perchlorate anions, and one water molecule of crystallization. The number of the perchlorate anion confirms that the complex cation is trivalent. The structure of the complex cation (+)₃₄₀^{CD}-[4a]³⁺ is shown in Figure 6, and its selected bond distances and angles are listed in Table 5. The complex cation (+)₃₄₀^{CD}-[4a]³⁺ consists of [Co(aet)₂(pymt)] and [Co(aet)₂(en)]⁺ octahedral units, which are bound to a Pt atom through aet S atoms to give a linear-type S-bridged trinuclear structure in [Pt{Co(aet)₂(en)}{Co(aet)₂(pymt)}]³⁺ (Pt1–Co1 = 3.343(1) Å, Pt1–Co2 = 3.341(1) Å, Co1–Pt1–Co2 = 173.45(4)°). The central PtS₄ sphere in (+)₃₄₀^{CD}-[4a]³⁺ is slightly distorted from square planar to tetrahedral geometry with the dihedral angle between S1–Pt1–S2 and S3–Pt1–S3 planes being 12.4°. A similar distortion of the PtS₄ sphere has been observed for [Pt{Co(aet)₂(en)}₂]⁴⁺, in which the dihedral angle is 13.1°.⁷ In (+)₃₄₀^{CD}-[4a]³⁺, the [Co(aet)₂(pymt)] unit adopts the *mer*(*S*)·*trans*(*N*_{aet}) configuration, as does the [Co(aet)₂(pyt)] unit in $\Delta\Delta$ -[1]²⁺, while the [Co(aet)₂(en)]⁺ unit has the normal *C*₂-*cis*(*S*) configuration. The noncentrosymmetric space group *P*2₁2₁2₁ implies that the

Table 5. Selected Bond Distances (Å) and Angles (deg) for $\Delta\Delta$ -[4](ClO₄)₃·H₂O

Distances			
Pt1–S1	2.311(3)	Co1–N5	1.987(9)
Pt1–S2	2.319(3)	Co1–N6	1.969(9)
Pt1–S3	2.315(3)	Co2–S3	2.269(3)
Pt1–S4	2.326(3)	Co2–S4	2.252(3)
Co1–S1	2.244(3)	Co2–S5	2.310(3)
Co1–S2	2.257(3)	Co2–N3	1.927(10)
Co1–N1	1.976(8)	Co2–N4	1.966(9)
Co1–N2	1.982(8)	Co2–N7	1.950(9)
Angles			
S1–Pt1–S2	84.36(10)	S3–Co2–N4	86.7(3)
S3–Pt1–S4	84.70(10)	S4–Co2–N3	87.3(3)
S1–Co1–S2	87.4(1)	S5–Co2–N7	72.1(3)
S1–Co1–N1	87.2(3)	Pt–S1–Co1	94.4(1)
S2–Co1–N2	87.0(3)	Pt–S2–Co1	93.8(1)
N5–Co1–N6	84.5(4)	Pt–S3–Co2	93.6(1)
S3–Co2–S4	87.5(1)	Pt–S4–Co2	93.7(1)

crystal of (+)₃₄₀^{CD}-[4a](ClO₄)₃·H₂O used for X-ray analysis consists of only one enantiomer: the absolute configuration was determined to be Δ for both the *C*₂-*cis*(*S*)-[Co(aet)₂(en)]⁺ and *mer*(*S*)-*trans*(*N*_{aet})-[Co(aet)₂(pymt)] units, based on the Flack parameter (0.0099(1)).¹⁵

The overall structure of $\Delta\Delta$ -[4]³⁺ ((+)₃₄₀^{CD}-[4a]³⁺) is similar to that of $\Delta\Delta$ / $\Lambda\Lambda$ -[Pt{Co(aet)₂(en)}₂]⁴⁺, except that one terminal en ligand is replaced by pymt. In particular, the bond distances and angles concerning the *C*₂-*cis*(*S*)-[Co(aet)₂(en)]⁺ unit in $\Delta\Delta$ -[4]³⁺, as well as the conformation of three chelate rings, are quite similar to those in $\Delta\Delta$ / $\Lambda\Lambda$ -[Pt{Co(aet)₂(en)}₂]⁴⁺.⁷ No significant difference in the Co–S_{aet} bond distances is observed between the *mer*(*S*)·*trans*(*N*_{aet})-[Co(aet)₂(pymt)] and *C*₂-*cis*(*S*)-[Co(aet)₂(en)]⁺ units in $\Delta\Delta$ -[4]³⁺. Moreover, the four Pt–S bond distances in $\Delta\Delta$ -[4]³⁺ fall within a small range (2.311(3)–2.326(3) Å), which are in good agreement with those in $\Delta\Delta$ / $\Lambda\Lambda$ -[Pt{Co(aet)₂(en)}₂]⁴⁺ (average 2.314(2) Å).^{4,7} Thus, it is seen that the introduction of pymt ligand in place of en little affects the Co–S_{aet} and Pt–S_{aet} bonds. In $\Delta\Delta$ -[4]³⁺, the Co–S_{pymt} (2.310(3) Å) and Co–N_{pymt} (1.950(9) Å) distances are slightly larger than the corresponding distances in *mer*(*S*)-[Co(pymt)₃] (Co–S = 2.289(5) Å, Co–N = 1.90(2) Å),^{14b} which seems to indicate that the pymt ligand in the *mer*(*S*)·*trans*(*N*_{aet})-[Co(aet)₂(pymt)] unit chelates to the Co^{III} center more weakly than does the pymt ligand in [Co(pymt)₃].

Formation Ratios of Homochoiral to Heterochoiral Forms.

Both the $\Delta\Delta$ (*meso*) and $\Delta\Delta$ / $\Lambda\Lambda$ (*racemic*) forms were produced for the present S-bridged Co^{III}Pt^{II}Co^{III} trinuclear complexes, [Pt{Co(aet)₂(pyt)}₂]²⁺ (**1**)²⁺ and [Pt{Co(aet)₂(en)}{Co(aet)₂(pyt)}]³⁺ (**2**)³⁺, which is in contrast to the selective formation of the $\Delta\Delta$ / $\Lambda\Lambda$ form for the corresponding Co^{III}Pd^{II}Co^{III} trinuclear complexes, [Pd{Co(aet)₂(pyt)}₂]²⁺ and [Pd{Co(aet)₂(en)}{Co(aet)₂(pyt)}]³⁺.⁸ A similar difference in the formation of the $\Delta\Delta$ and $\Delta\Delta$ / $\Lambda\Lambda$ forms has been recognized between the analogous S-bridged Co^{III}Pt^{II}Co^{III} and Co^{III}Pd^{II}Co^{III} trinuclear complexes composed of two *C*₂-*cis*(*S*)-[Co(aet)₂(en)]⁺ units, [M{Co(aet)₂(en)}₂]⁴⁺ (M = Pd^{II},

(14) (a) Constable, E. C.; Palmer, C. A.; Tocher, D. A. *Inorg. Chim. Acta* **1990**, *176*, 57–60. (b) Jung, O.-S.; Kim, Y. T.; Kim, Y. J.; Chon, J.-K.; Chae, H. K. *Bull. Korean Chem. Soc.* **1999**, *20*, 648–652.

(15) (a) Flack, H. D. *Acta Crystallogr., Sect. A* **1983**, *39*, 876–881. (b) Flack, H. D.; Bernardinello, G. *Acta Crystallogr., Sect. A* **1985**, *41*, 500–511.

Pt^{II}), which has been explained by a combination of thermodynamic stability of $\Delta\Delta/\Lambda\Lambda$ form vs $\Delta\Lambda$ form and kinetic lability of Pd–S bond vs Pt–S bond.⁷ That is, the thermodynamically unstable $\Delta\Lambda$ form created at the first stage converts to the $\Delta\Delta/\Lambda\Lambda$ form for M = Pd^{II} because of the kinetic lability of the Pd–S bond, while the inertness of Pt–S bond prevents the $\Delta\Lambda$ form from converting to the $\Delta\Delta/\Lambda\Lambda$ form for M = Pt^{II} to afford both the $\Delta\Lambda$ and $\Delta\Delta/\Lambda\Lambda$ forms. It is noticed that, however, the formation ratio of $\Delta\Lambda:\Delta\Delta/\Lambda\Lambda$ for [1]²⁺ was ca. 1:3, which is different from a ca. 1:1 ratio observed for [Pt{Co(aet)₂(en)}₂]⁴⁺. Furthermore, the formation ratio of $\Delta_{\text{en}}\Lambda_{\text{pyt}}/\Lambda_{\text{en}}\Delta_{\text{pyt}}:\Delta\Delta/\Lambda\Lambda$ for [2]³⁺ was ca. 1:2, which is intermediate between the ca. 1:3 ratio of $\Delta\Lambda:\Delta\Delta/\Lambda\Lambda$ for [1]²⁺ and the ca. 1:1 ratio of $\Delta\Lambda:\Delta\Delta/\Lambda\Lambda$ for [Pt{Co(aet)₂(en)}₂]⁴⁺. These results point out that the introduction of pyt in place of en induces the preferential formation of the $\Delta\Delta/\Lambda\Lambda$ form. When pytm is introduced in place of en in [Pt{Co(aet)₂(en)}₂]⁴⁺, a remarkable predominant formation of the $\Delta\Delta/\Lambda\Lambda$ form was recognized; the formation ratio of $\Delta\Lambda$ to $\Delta\Delta/\Lambda\Lambda$ for [Pt{Co(aet)₂(pytm)}₂]²⁺ ([3]²⁺) was evaluated to be less than 1:10. Notably, the predominant formation of the $\Delta\Delta/\Lambda\Lambda$ form was also found for [Pt{Co(aet)₂(en)}{Co(aet)₂(pytm)}]³⁺ ([4]³⁺), in which only one of two terminal en ligand in [Pt{Co(aet)₂(en)}₂]²⁺ is replaced by pytm. Thus, the preferential formation of the $\Delta\Delta/\Lambda\Lambda$ form is dramatically increased by the introduction of pytm at the terminal of the S-bridged Co^{III}Pt^{II}Co^{III} trinuclear structure.

One may assume that the Pt–S bonds in the trinuclear structure are weakened by the replacement of the terminal en ligands by pyt or pytm ligands, which allows the intermolecular exchange of the [Co(aet)₂(pyt or pytm)] units to form the more stable $\Delta\Delta/\Lambda\Lambda$ form. However, the Pt–S bond distances in $\Delta\Delta/\Lambda\Lambda$ - and $\Delta\Lambda$ -[Pt{Co(aet)₂(en)}₂]⁴⁺, $\Delta\Lambda$ -[Pt{Co(aet)₂(pyt)}₂]²⁺ ($\Delta\Lambda$ -[1]²⁺), and $\Delta\Lambda$ -[Pt{Co(aet)₂(en)}{Co(aet)₂(pytm)}]³⁺ ($\Delta\Lambda$ -[4]³⁺) are quite similar to one another. Furthermore, the reactions of a 1:1 mixture of [Ni{Co(aet)₂(pyt or pytm)}₂]²⁺ and [Ni{Co(aet)₂(en)}₂]⁴⁺ with Pt^{II} followed an almost statistical distribution to give [Pt{Co(aet)₂(pyt or pytm)}₂]²⁺, [Pt{Co(aet)₂(en)}{Co(aet)₂(pyt or pytm)}]³⁺, and [Pt{Co(aet)₂(en)}₂]⁴⁺ in a ratio of ca. 1:2:1. These facts suggest that the binding ability of aet thiolato groups in [Co(aet)₂(pyt)], [Co(aet)₂(pytm)], and [Co(aet)₂(en)]⁺ toward Pt^{II} ion are comparable to each other. Thus, the remarkable variation of the formation ratio for the S-bridged Co^{III}Pt^{II}Co^{III} complexes seems to be ascribed to the difference in the stability of [Co(aet)₂(L)]⁺ or ⁰ (L = en, pyt, pytm) toward isomerization, which is affected by the choice of the terminal bidentate ligand L. That is, in the course of the metal replacement reaction, the [Co(aet)₂(pyt)] unit having the strained four-membered pyt chelate ring would suffer isomerization more easily than the [Co(aet)₂(en)]⁺ unit so as to generate the more stable $\Delta\Delta/\Lambda\Lambda$ form, which results in the preferential formation of the $\Delta\Delta/\Lambda\Lambda$ form in the final product. The lower stability of the [Co(aet)₂(pyt)] unit is indicated by the d–d absorption band for $\Delta\Delta/\Lambda\Lambda$ -[Pt{Co(aet)₂(pyt)}₂]²⁺ ($\Delta\Delta/\Lambda\Lambda$ -[1]²⁺), which locates at considerably lower energy than the corresponding

band for $\Delta\Delta/\Lambda\Lambda$ -[Pt{Co(aet)₂(en)}₂]⁴⁺ (Figure 1 and Table 2). Furthermore, the introduction of pytm, which is assumed to have a binding ability weaker than that of pyt (because of the presence of uncoordinated, electron-withdrawing nitrogen atom), would much facilitate the isomerization of the octahedral units, leading to the predominant formation of the $\Delta\Delta/\Lambda\Lambda$ form. It has been recognized that [Ni{Co(aet)₂(pytm)}₂]²⁺ shows an absorption spectral change with time in water much faster than does [Ni{Co(aet)₂(pyt)}₂]²⁺.⁸ This may support the lower stability of the [Co(aet)₂(pytm)] unit, compared with the [Co(aet)₂(pyt)] unit, along with the fact that $\Delta\Delta/\Lambda\Lambda$ -[Pt{Co(aet)₂(pytm)}₂]²⁺ ($\Delta\Delta/\Lambda\Lambda$ -[3]²⁺) exhibits the d–d absorption band at lower energy than the d–d band for $\Delta\Delta/\Lambda\Lambda$ -[Pt{Co(aet)₂(pyt)}₂]⁴⁺ ($\Delta\Delta/\Lambda\Lambda$ -[1]²⁺) (Table 2).

Concluding Remarks

In this study, a series of S-bridged Co^{III}Pt^{II}Co^{III} trinuclear complexes, [Pt{Co(aet)₂(pyt)}₂]²⁺ ([1]²⁺), [Pt{Co(aet)₂(en)}{Co(aet)₂(pyt)}]³⁺ ([2]³⁺), [Pt{Co(aet)₂(pytm)}₂]²⁺ ([3]²⁺), and [Pt{Co(aet)₂(en)}{Co(aet)₂(pytm)}]³⁺ ([4]³⁺), were newly prepared by the use of [Ni{Co(aet)₂(L)}₂]⁴⁺ or ²⁺ (L = en, pyt, pytm) as sources of the octahedral [Co(aet)₂(L)]⁺ or ⁰ units, and the homochiral ($\Delta\Delta/\Lambda\Lambda$) and heterochiral ($\Delta\Lambda$) forms produced were successfully separated and optically resolved. While the $\Delta\Delta/\Lambda\Lambda$ and $\Delta\Lambda$ forms are almost equally generated for [Pt{Co(aet)₂(en)}₂]⁴⁺, the preferential formation of the $\Delta\Delta/\Lambda\Lambda$ form was recognized for [1]²⁺ and [2]³⁺ containing the [Co(aet)₂(pyt)] unit. Furthermore, it was found that the introduction of the [Co(aet)₂(pytm)] unit in the trinuclear structure results in the remarkable predominant formation of the $\Delta\Delta/\Lambda\Lambda$ form for [3]²⁺ and [4]³⁺, although the spectroscopic and structural properties of [3]²⁺ and [4]³⁺ are similar to those of [1]²⁺ and [2]³⁺. These results first show that the homochiral vs heterochiral linkages of tris(chelate)-type complex units could be controlled by the choice of appropriate coligand, which does not bridge two metal centers. It should be noted that the additivity on CD was successfully applied to assign the chiral configuration for the present S-bridged Co^{III}Pt^{II}Co^{III} trinuclear system. Thus, the configurational assignment of optically active isomers of other coordination systems, such as discrete polynuclear complexes and dimensional coordination polymers, could be made by the CD curve analysis, based on the assumption that the CD contributions from several chiral centers are additive. Finally, the present results obtained from the relatively simple trinuclear system would provide basic and significant information that contributes to the development of chiral selective construction of polynuclear systems.

Acknowledgment. This work was partially supported by a Grant-in-Aid for Scientific Research on Priority Areas (No. 14078101) from the Ministry of Education, Culture, Sports, Science, and Technology of Japan.

Supporting Information Available: X-ray crystallographic files, in CIF format, for the structure determination of $\Delta\Lambda$ -[1]Cl₂·4H₂O and $\Delta\Lambda$ -[4](ClO₄)₃·H₂O. This material is available free of charge via the Internet at <http://pubs.acs.org>.

IC0303338